ISBN: 978-3-95450-197-7 doi:10.18429/JACoW-RUPAC2018-THCBMH02

EVALUATIONS OF PARAMETERS STABILITY FOR S-BAND RF GUN CAVITY DUE TO EFFECTS OF PULSED RF HEATING

V. Paramonov*, A. Skasyrskaya, INR of the RAS, 117312, Moscow, Russia
B.L. Militsyn, UKRI STFC/ASTeC, Daresbury, Warrington, Cheshire, UK

Abstract

Requirements to high stability of electron beam arrival time in modern FEL facilities transform to requirements of high stability of amplitude and phase of electric fied in RF photocathode gun which is used as electron injector. To provide high quality of bunches, gun cavities with high electric and hence magnetic RF fields. Effects, related to pulse RF heating, result in change of the cavity frequency and quality factor during even few μs RF pulse. Cavity deformations due to pulse heating are considered and corresponding cavity detuning are evaluated. Resulting deviations of the phase and amplitude of the RF field in the gun cavity as a function of RF pulse duration are estimated.

INTRODUCTION

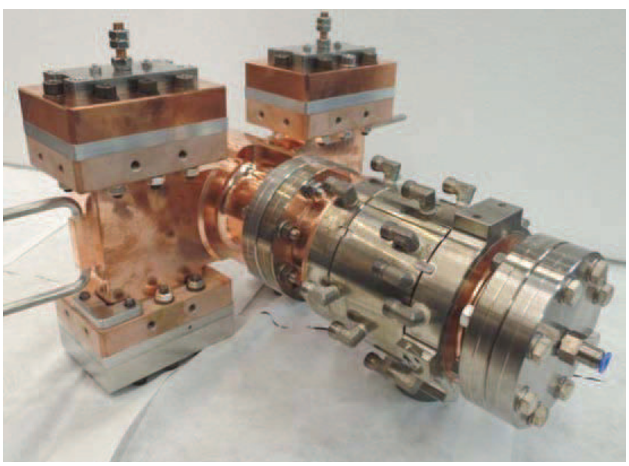

Figure 1: S band HRRG RF cavity for the CLARA project.

Photocathode RF guns are now widely used for generation of short and bright electron beams in modern Free Electron Laser (FEL) facilities. For low repetition rate FEL the guns are usually based on S-band normal conducting RF cavities. Despite of specific requirements to different facilities and details of technical decisions used, design and operating mode of the gun cavities have common, typical patterns. As a typical modern example Fig. 1 illustrates High Repetition Rate Gun (HRRG) photocathode gun designed for the CLARA project, [1]. HRRG 1.5 cell cavity has a coaxial input RF coupler with symmetric feed.

To provide electron bunches with small transverse emittance the gun operate in pulsed mode with a high, of up to $\sim 120\ \frac{MV}{m}$ electric field E_c at the cathode surface. With a need it results in a high, of $\sim 250\ \frac{kA}{m}$ magnetic field at the surface H_m and the high density of the pulsed RF losses P_s of up to $\sim 4.5 \cdot 10^8 \frac{W}{m^2}$. Effects of the pulsed RF heating take place during RF pulse $\tau \sim (3 \div 6)\ \mu s$ then the temperature at some parts of the cavity surface T_s rises up to $(19 \div 30)\ C^o$.

One of the critical requirements to the linear accelerator based FEL facilities with laser seeding is high arrival time stability of the electron bunches. Essential impact on the arrival time gives the amplitude and phase of the pulsed RF field in the gun cavity, [2]. Temperature rise of the cavity during RF pulse leads to thermal deformations and change of the cavity parameters. It directly lead to deviations in the amplitude and the phase of the RF field in the cavity.

PROCESS DESCRIPTION

Process of thermal elastic deformations is described by the coupled equations for temperature $T(\vec{r},t)$ and displacements $\vec{u}(\vec{r},t)$ distributions, [3]:

$$div(gradT(\vec{r},t)) - \frac{\rho_m C_p}{k_c}\frac{\partial T(\vec{r},t)}{\partial t} - \\ - \frac{\alpha_t E_Y T_0}{3k_c(1-2\nu)}\frac{\partial div\vec{u}}{dt} = 0,$$

$$\frac{3(1-\nu)}{(1+\nu)} grad(div\vec{u}) - \frac{3(1-2\nu)}{2(1+\nu)} rotrot\vec{u} - \\ -\alpha_t gradT(\vec{r},t) - \frac{3(1-2\nu)\rho_m}{E_y}\frac{\partial^2 \vec{u}}{\partial t^2} = 0, \quad (1)$$

where $\rho_m, C_p, k_c, \alpha_t, E_Y$ and ν are the density, the specific heat, the heat conductivity, the coefficient of linear thermal expansion, the Young's modulus and the Poisson ratio, respectively. The first equation in Eq. 1 describes the heat diffusion from the heated surface into the cavity body. This process is well studied and explained in [4] and related references. The pulsed temperature rise T_s of the surface over the average steady-state value and the heat penetration depth into body D_d can be estimated as:

$$T_s = \frac{2P_s\sqrt{\tau}}{\sqrt{\pi k_c \rho_m C_p}}, \quad \alpha_d = \frac{k_c \tau}{\rho_m C_p}, \quad D_d = \sqrt{\alpha_d \tau}, \quad (2)$$

where $\alpha_d \approx 10^{-4}\ \frac{m^2}{s}$ is the thermal diffusivity for copper. For the RF pulse duration $\tau = 1\ \mu s,\ 3\ \mu s,\ 6\ \mu s$ and $10\ \mu s$ the heat penetrates to the depth $D_d = 10.7\ \mu m,\ 18.5\ \mu m,\ 26.2\ \mu m$ and $33.8\ \mu m$ respectively.

The second equation in Eq. 1 is a typical wave equation for displacements $\vec{u}$ with source $\alpha_T gradT(\vec{r},t)$. Equation describes propagation of longitudinal elastic waves of compression from the source with velocity $V_l =$

* paramono@inr.ru

ISBN: 978-3-95450-197-7 doi:10.18429/JACoW-RUPAC2018-THCBMH02

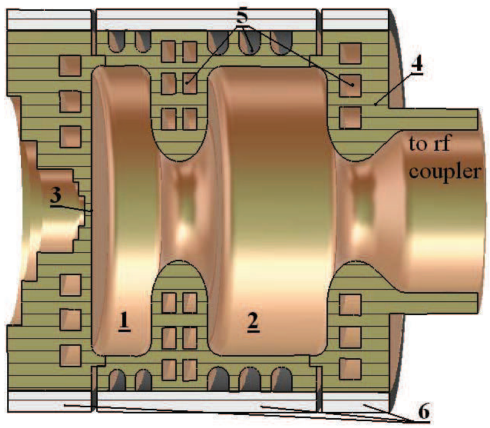

Figure 2: Simplified model of the gun cavity. 1 - half cathode cell, 2 - full cell, 3 - position of photo cathode, 4- cavity copper body, 5 - cooling channels, 6 - stainless steel jacket.

$\sqrt{\frac{E_y(1-\nu)}{2\rho_m(1+\nu)(1-2\nu)}} \approx 4700\ \frac{m}{s}$. The real cavity design, Fig. 1, contains a lot of technical elements. We have to consider simplified cavity model, taking into account exclusively essential components, Fig. 2. Even for such simplified model we can obtain results with direct numerical simulations only by using certified software like ANSYS, [5]. Coupled Eq. 1 describe two processes that differ by five orders of magnitude in the propagation velocities - diffusive heat propagation with a velocity of $\approx 10^{-2}\ \frac{m}{s}$ and elastic wave propagation with velocity $V_l \sim 4.5 \cdot 10^3\ \frac{m}{s}$. Typical distance between the cavity surface and a violation of the cavity body homogeneity - cooling channels - is of $\sim 3\,mm$, Fig. 2. The travel time of elastic wave from the inner surface to channel and back about of $\approx 1.2\ \mu s$ and is shorter than RF pulse duration. During RF pulse we should expect interaction of the forward wave from the inner cavity surface with backward waves, reflected from violations of cavity body homogeneity.

The heated surface layer is rather thin as compared to the typical cavity dimensions. The main problem in numerical simulations is to describe precisely both the rapidly falling temperature distribution in the bulk of the cavity and also rapidly falling distribution of the first derivative $\alpha_t gradT(\vec{r}, t)$ - a source in the equation for elastic waves Eq. 1. For numerical simulations the procedure was used originally developed for pulsed RF heating simulations in L-band gun cavities, operating with much longer RF pulse $\sim 800\mu s$, [6], but with significant changes to describe much thinner hot layer in the S-band case.

The procedure has been thoroughly verified on simple models of hollow spherical cavities, which allow an analytic solutions for displacements in Eq. 1 in some approximations [3]. For the cost of computing resources and considering only 30 degree sector of simplified model, Fig. 2, the deviations between analytic and numerical results in units of percents was achieved and procedure parameters were fixed for further simulations. Materials parameters $\rho_m, C_p, k_c, \alpha_t, E_Y$ and ν, required for numerical simulations, accepted assuming typically used in cavities construction materials - OFE annealed copper and AISI steel, as listed in [7].

NUMERICAL RESULTS

Both rectangular ($P_l = P_s = const, 0 \leq t \leq \tau$, to compare T_s with Eq. 2) and accretive ($P_l = P_s(1-e^{-\frac{t}{\tau_c}})^2, 0 \leq t \leq \tau$) pulsed heat loads P_l were considered, where τ_c is the filling time of the cavity. For a short pulse $\tau \sim (3 \div 6)\mu s$ the accretive shape of the heat load P_l is essential and two options $\tau_{c1} = 0.62\mu s$ and $\tau_{c2} = 0.76\mu s$ were considered for comparison.

For rectangular P_l pulse the estimations based on Eq. 2 for T_s works fine. All the time, with the precision of D_d, distribution T_s reflects the surface distribution of P_s. In Fig. 3a maximal surface temperature evolutions T_{smax} for different P_l pulses are shown assuming the maximal RF loss density of $P_{smax} = 4.48 \cdot 10^8\ \frac{W}{m}$. Thickness of the hot layer $\sim D_d$ strongly exceeds the thickness of the RF skin layer $\delta \sim 0.9\mu m$ and temperature rise at the surface results in the increasing of the surface resistance and an additional growth of RF losses dP. Large T_s rise which is due to the surface resistance increasing takes place in the cavity parts with high magnetic fields. The effect of losses increasing for pulsed RF heating is more pronounced. As T_s rise is not that big as compared to absolute surface temperature, time dependence of additional RF losses, illustrated in Fig. 3b, are similar to dynamics of of T_s.

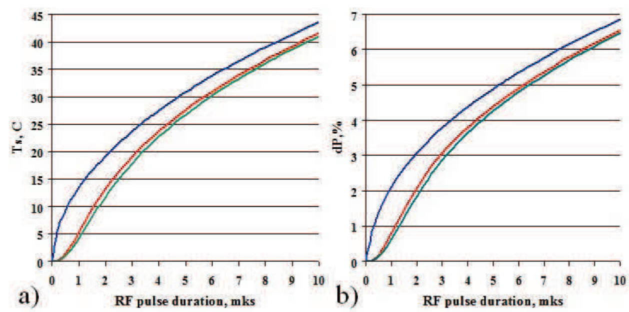

Figure 3: Time dependence of maximal temperature rise of the surface T_{smax} (a) and relative increase of RF losses (b) for rectangular (blue traces) and accretive with τ_{c1} (red traces) or τ_{c2} (green traces) P_l pulse.

For long RF pulse in L-band gun cavities we can consider distribution of displacements as steady-state, neglect-

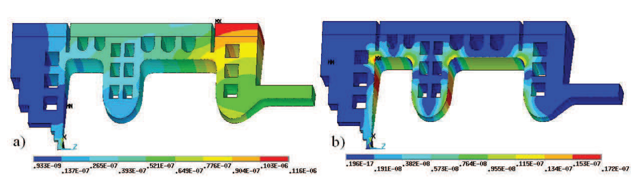

Figure 4: Distribution of displacements after $\tau = 4.5\ \mu s$ accretive (τ_{c1}) RF pulse for static (a) and transient (b) approximations.

ISBN: 978-3-95450-197-7 doi:10.18429/JACoW-RUPAC2018-THCBMH02

ing terms $\frac{\partial div\vec{u}}{dt}$ and $\frac{\partial^2\vec{u}}{\partial t^2}$ in Eq. 1. It means the assumption of infinite velocity of elastic waves propagation. For the short pulses in S-band cavities this assumption leads to not correct results. Figure 4 shows distributions of displacements in the cavity after $\tau = 4.5\ \mu s$ accretive (τ_{c1}) P_l pulse for static and transient approximations. With the similar maximal values of $\approx 0.15\ \mu m$, spatial $\vec{u}$ distributions are very different. It results in quite different values of displacements for cavity surface and related resonance frequency shift df. Figure 5a depicts the qualitative difference in frequency shifts, calculated in static and transient approximations in dependence on RF pulse length. For different P_l pulses calculated transient df values are shown in Fig. 5b.

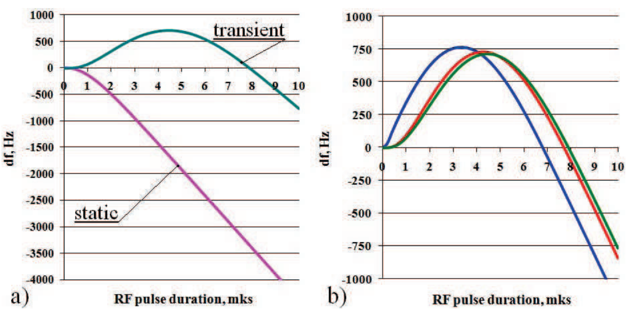

Figure 5: Cavity detuning during accretive (τ_{c1}) P_l pulse for static and transient approximations (a) and transient detuning for rectangular (blue curve), accretive with τ_{c1} (red curve) or τ_{c2} (green curve) P_l pulses (b).

IMPACT ON RF FIELD STABILITY

Amplitude A and phase ϕ of RF oscillations in the gun cavity depend on the frequency detuning df as:

$$A = A_0\sqrt{\frac{1-\rho_0^2}{1+(\frac{2Q_l df}{f_0})^2}}cos(\omega t-\phi), \phi = arctg(\frac{2Q_l df}{f_0}), \tag{3}$$

where Q_l and Q_0 are the loaded and own quality factors, $\rho_0 = 1 - \frac{2Q_l}{Q_0}$ is the initial reflections coefficient. For example, in the tuned HRRG gun cavity values $Q_0 = 12190$ and $Q_l = 5870$, [8], are typical for S-band gun cavities. For the maximal detuning $df \approx 700\ Hz$, see Fig. 5b, the normalized detuning is $\frac{2Q_l df}{f_0} \approx 2.7 \cdot 10^{-3}$.
The df contribution to amplitude A is in the second order and for obtained df values negligible. For the phase ϕ deviation df influence is in the first order. In Fig. 6a are shown plots of ϕ dependencies, corresponding to df plots in Fig. 5b. Increasing of RF losses due to surface temperature rise, Fig. 3b, naturally leads to decrease of own quality fac tor Q_0 during RF pulse. It results a change of cavity matching with RF coupler - variation in reflection coefficient ρ_0 and, according to Eq. 3, deviations in the field amplitude A For the field amplitude during RF pulse takes place a natural rise as $A = A_0 \cdot (1 - e^{-\frac{t}{\tau_c}})$ and corresponding deviation $|A_0 - A|$ is illustrated in Fig. 6b by the red dashed straight

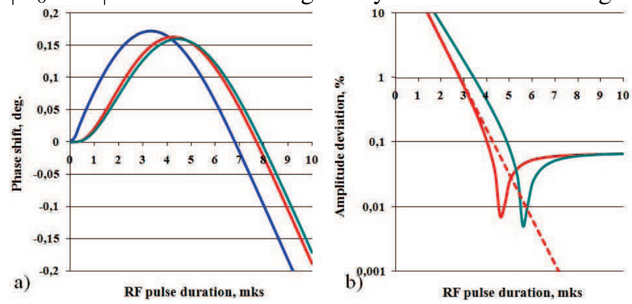

Figure 6: Temporal dependence of the phase shift of RF oscillations for rectangular (blue curve), accretive with τ_{c1} (red curve) or τ_{c2} (green curve) P_l pulses (a) and absolute value of amplitude deviations for accretive with τ_{c1} (red curve) or τ_{c2} (green curve) P_l pulses (b).

line. Related to the ρ_0 change $\sim \sqrt{1-\rho_0^2}$ amplitude deviation depends on the initial cavity matching. For the typical example under consideration dependences of amplitude deviations $|1 - \frac{A}{A_0}|$ on time are shown in Fig. 6b.

SUMMARY

For typical operating modes of S-band RF gun cavities the effects of pulsed heating during the the RF pulse are manifested not only in the growth of surface temperature but also in small but unavoidable thermal deformations. During a short RF pulse these deformations are essentially non-stationary. Both surface temperature rise and cavity thermal deformations result in changes of own quality factor and cavity resonance frequency even during few microseconds long RF pulse. This report presents results of numerical simulation of both the cavity parameters change and related deviations of the RF field amplitude and phase for typical operating regime.

ACKNOWLEDGEMENT

The work is supported by STFC contract N 4070193704.

REFERENCES

[1] D. Angal-Kalinin *et al.*, "Comissioning of Front End of CLARA Facility at Daresbury Laboratory", in *Proc. IPAC 2018*, Vancouver, Canada, p. 4426, 2018

[2] B.P.M. Liggins *et al.*, "Jitter Tolerance for CLARA", in *Proc. IPAC 2013*, SHanghai, China, p. 1271, 2013

[3] A.D. Kovalenko, *Introduction to thermo-elasticity*, Kiev, USSR, Naukova dumka, 1965

[4] D. Pritzkau and R. Siemann, "Experimental study of rf pulsed heating on OFE copper", *PRST Accel. Beams*, v. 5, p. 112002, 2002.

[5] ANSYS, `http://www.ansys.com`.

[6] V. Paramonov and A. Skasyrskaya, "Pulsed RF heating simulations ", DESY, Hamburg, TESLA-FEL 2007-04, 2007.

[7] V. Paramonov *et al.*, "Design of an L-band Normally Conducting RF Gun Cavity", *NIM A*, vol. 854, pp. 113-126, 2017.

[8] L.S. Cowie, private communication, 2018